

Phase transitions and glasslike behavior in $\text{Sr}_{1-x}\text{Ba}_x\text{TiO}_3$

V. V. Lemanov, E. P. Smirnova, P. P. Symnikov, and E. A. Tarakanov

A. F. Ioffe Physico-Technical Institute, 194021 St. Petersburg, Russia

(Received 16 October 1995; revised manuscript received 23 January 1996)

A dielectric and ultrasonic study of phase transitions in $\text{Sr}_{1-x}\text{Ba}_x\text{TiO}_3$ with x ranging from 0.0 to 1.0, is reported. Both ceramic samples and single crystals were studied. The full phase diagram is derived from dielectric measurements for ferroelectric phase transitions and from ultrasonic measurements for structural phase transition. The cubic-tetragonal ferroelectric phase transition which is of the first order in pure BaTiO_3 ($x=1.0$) transforms to the second order phase transition at x close to 0.2. The transition temperature T_c is a linear function of x at x values from 0.2 to 1.0. For $x < 0.2$ the transition temperature is proportional to $(x - x_c)^{1/2}$, where $x_c = 0.035$. For $x < x_c$ a glasslike behavior is observed. The structural phase transition temperature T_a goes down as compared to pure SrTiO_3 when x increases and levels off near $x=0.05$. [S0163-1829(96)08626-2]

I. INTRODUCTION

Ferroelectric solid solutions with perovskite structure have been a subject of extensive study since the early 1950s. In particular, many papers were devoted to BaTiO_3 - SrTiO_3 solid solutions (see Refs. 1–3 and references therein). However, the solid solutions with relatively high BaTiO_3 concentration x and at temperatures above 100 K were mainly studied. $\text{Sr}_{1-x}\text{Ba}_x\text{TiO}_3$ samples with low x and at low temperatures were measured by Hegenbarth,⁴ Miura *et al.*,⁵ and Bednorz,⁶ but their works do not give a full picture of phase transitions in this system. In the present paper we report the detailed study of $\text{Sr}_{1-x}\text{Ba}_x\text{TiO}_3$ solid solutions, using both ceramic samples and single crystals in the whole range of x from $x=0.0$ to 1.0. Some preliminary results on dielectric study of ceramic samples of this system have been published elsewhere.⁷

The dielectric and ultrasonic measurements were used in the present paper to study ferroelectric and structural phase transitions and to derive the full phase diagram of the SrTiO_3 - BaTiO_3 system. Main attention was focused on solid solutions with small x , that is on the SrTiO_3 side. It is well known that SrTiO_3 is an incipient ferroelectric in which ferroelectric phase transition is suppressed by quantum fluctuations.⁸ A small amount of impurities can, in principle, induce such transitions with an intermediate glasslike state similar to KTaO_3 with a small concentration of KNbO_3 (KTN) or LiTaO_3 (KTL). Thus the general aim of our study was to find peculiarities, if any, in the phase transition picture for the SrTiO_3 - BaTiO_3 system with a special attention to the relatively low BaTiO_3 concentration.

The paper is organized as follows. The sample preparation and the experimental techniques are described in Sec. II. The experimental results are presented in Sec. III. Section IV is devoted to the phase diagram of the $\text{Sr}_{1-x}\text{Ba}_x\text{TiO}_3$ system as deduced from the dielectric and ultrasonic measurements. Three different ranges of x are considered here: (A) $0.15 < x < 1.0$, (B) $0.035 < x < 0.2$, and (C) $0 < x < 0.035$ (glasslike behavior). In Sec. IV D the structural phase transition studied with an ultrasonic technique is considered. The discussion of

all the results is given in Sec. V. The summarized results and the conclusions are presented in Sec. VI.

II. EXPERIMENTAL PROCEDURES

For the preparation of $\text{Sr}_{1-x}\text{Ba}_x\text{TiO}_3$ ceramic samples a conventional ceramic technology was used.¹ Starting chemical materials were BaCO_3 , TiO_2 , and SrCO_3 (99.9% purity).

$\text{Sr}_{1-x}\text{Ba}_x\text{TiO}_3$ single crystals were grown by a flux method. KF-LiF mixture was chosen as a flux which we consider to be the best one for this system. The obtained single crystals had dimensions up to $2 \times 2 \times 2$ mm³. For dielectric measurements thin plates with thickness about 0.5 mm were used. The normal to the plates was along the $\langle 100 \rangle$ type pseudocubic direction.

The dielectric constant ϵ was measured at the frequencies 10^2 , 10^3 , 10^4 , and 10^6 Hz using automatic capacitance bridges. The amplitude of an ac electric field in dielectric measurements was about 10 V/cm. As electrodes we used silver paste which was burnt into the samples at 500 °C.

For ultrasonic study an echo-pulse method was used. The pulse duration was about 10^{-6} s. Longitudinal ultrasonic waves with the frequency of 10 MHz were excited and detected with LiNbO_3 thin-plate transducers. The ultrasonic wave velocity v was measured by the pulse superposition method with an accuracy about 10^{-4} . Only ceramic samples with the dimensions about $4 \times 4 \times 6$ mm³ were studied with the ultrasonic technique.

All the measurements were carried out in the temperature region from 4.2 up to 420 K. In the low-temperature measurements a He-flow cryostat was used.

III. EXPERIMENTAL RESULTS

An x-ray-diffraction study showed that all the samples were single-phase perovskite solid solutions. The lattice parameters of the ceramic samples were measured at room temperature as a function of x for x from 0.0 to 1.0. At room temperature the samples are cubic for $x < 0.7$ and tetragonal ($a = b \neq c$) for $x > 0.7$. The lattice parameter increases with increasing x practically by a linear Vegard law: $\Delta a = 0.1x$ (Å) where Δa is the increment of the SrTiO_3 lattice parameter in

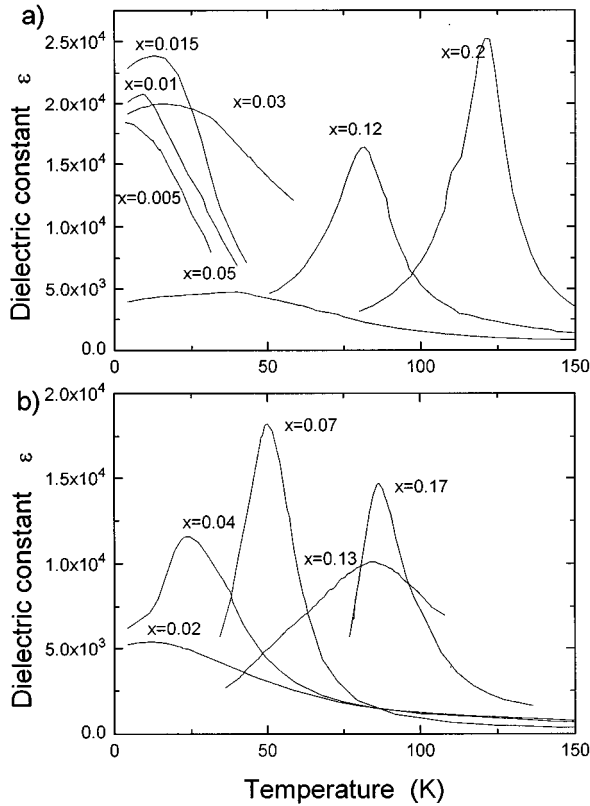


FIG. 1. Temperature dependence of dielectric constant at frequency of 1 kHz in ceramics (a) and single crystals (b). (The numbers near the curves refer to BaTiO₃ concentration x .)

a sample with BaTiO₃ concentration x [for $x > 0.7$ the average lattice parameter $\bar{a} = (a^2c)^{1/3}$ is taken].

The concentration x in the single crystals was determined by measuring the lattice parameter a and using the experimental dependence of a versus x for the ceramic samples. We estimate an absolute accuracy of this determination of x as about 1%.

Some results of the dielectric measurements are shown in Fig. 1. The temperature dependence of the dielectric constant ϵ at the frequency of 1 kHz is presented here for ceramics [Fig. 1(a)] and single crystals [Fig. 1(b)].

For $x \geq 0.3$, one can observe three maxima of the dielectric constant which correspond to three phase transitions: a large maximum for the high-temperature $m3m-4mm$ phase transition, and two small maxima for the low-temperature $4mm-mm2$ and $mm2-3m$ phase transitions. The two low-temperature maxima are very distinct at $x = 1.0$ and disappear gradually when x decreases. As seen from Fig. 1(a), at $x = 0.2$ along with the main maximum there is only a small “shoulder” on the low-temperature side of ϵ versus T dependence.

The temperature dependence of the dielectric constant for the single crystals [Fig. 1(b)] within the experimental errors gives the same temperature positions of the dielectric constant maxima as for the ceramic samples.

The maximum value of the dielectric constant ϵ_m for the single crystals is generally either equal or about a factor 1.5 smaller than for the ceramic samples. The only exception is the single crystal with $x = 0.07$. For this sample ϵ_m is two times larger than for the ceramic samples with the same x .

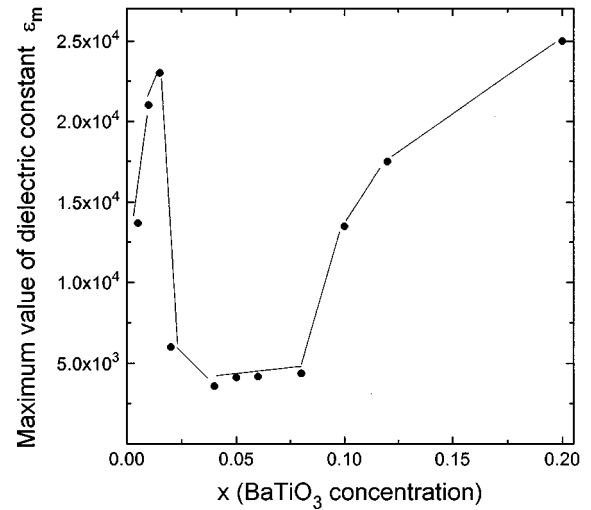


FIG. 2. Maximum value of dielectric constant in ceramic samples as a function of BaTiO₃ concentration x at frequency of 1 kHz.

This scatter of the ϵ_m values may be due to the different quality of our single crystals.

The ϵ_m as a function of x for the ceramic samples is shown in Fig. 2. Within the $x = 1.0-0.2$ range, not shown in Fig. 2, the dielectric constant ϵ_m grows from about 10^4 at $x = 1.0$ up to 2.5×10^4 at $x = 0.2$.

The phase transitions in pure BaTiO₃ are known to be of the first order, that is a temperature hysteresis is a characteristic feature of these transitions. It turned out that for the high-temperature $m3m-4mm$ phase transition the hysteresis, determined as $\Delta T = T_c^+ - T_c^-$, where T_c^+ and T_c^- are the ϵ_m temperatures for heating and cooling runs, respectively, decreases with x decreasing and vanishes ($\Delta T = 0$) at $x = 0.2-0.25$ (Fig. 3). We estimate an error in the determination of the hysteresis as about 0.5 K. This result is in general agreement with available data⁹ though our value of x where $\Delta T = 0$ is somewhat smaller.

It was interesting, as always for solid solutions, to find out whether there is a frequency dispersion of the dielectric constant. The measurements showed that the frequency dispersion of ϵ does exist but only for small values of x (Fig. 4). For example, at $x = 0.02$ the difference between T_m at 10^6 and

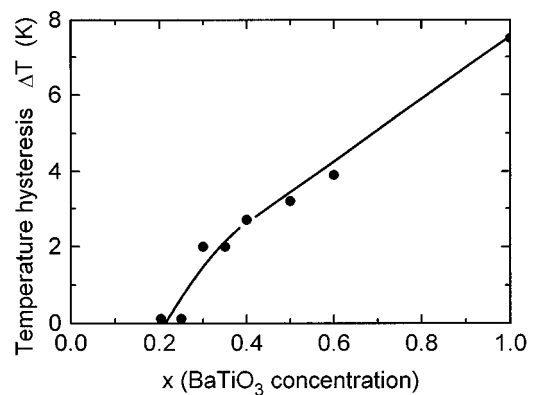


FIG. 3. Temperature hysteresis $\Delta T = T_c^+ - T_c^-$ for the $m3m-4mm$ phase transition versus BaTiO₃ concentration x .

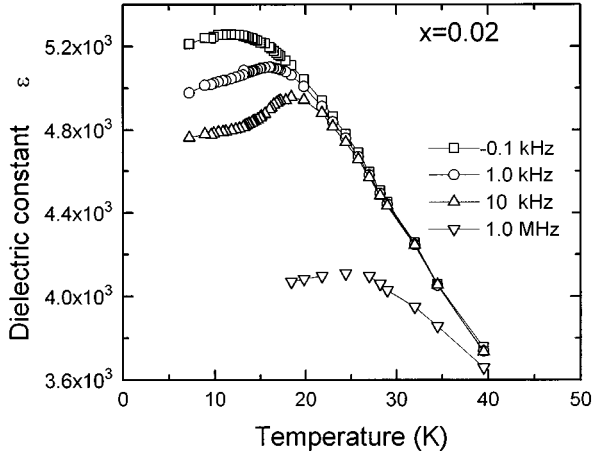


FIG. 4. Temperature dependence of dielectric constant at different frequencies in single crystal with $x=0.02$.

10^2 Hz reaches 13 K for single crystals and becomes zero for x in the region of 0.15–0.20 (Fig. 5). For the ceramic samples this difference appears to be about one-half of that for the single crystals. The decrease of the dispersion at $x < 0.015$ seems to be due to the approaching pure SrTiO_3 , which has no frequency dispersion of dielectric constant in this frequency range.

Ferroelectric hysteresis loops were measured using a conventional Sawyer-Tower circuit at temperatures $T > T_m$ and $T < T_m$, where T_m is the temperature of the dielectric constant maximum. For $x > 0.03$ the typical ferroelectric hysteresis loops were observed at $T < T_m$ [Fig. 6(a)], while for $x < 0.03$ no hysteresis loops were observed [Fig. 6(b)].

Having in mind the possibility of a long-term dielectric relaxation for samples with a large frequency dispersion of ϵ , we measured the relaxation effects in the samples with $x=0.02$. The results of this experiment are shown in Fig. 7. The samples were field cooled down to 10 K in a dc electric field of 1 kV/cm, then at time $t=0$ the electric field was switched off, and the ϵ versus t dependence was measured. Indeed, the long-term relaxation was observed, with ϵ decreasing by about 10% in the time interval about 10^3 s.

In pure SrTiO_3 the well-known structural phase transition (improper ferroelastic transition $m3m-4/mmm$) occurs at

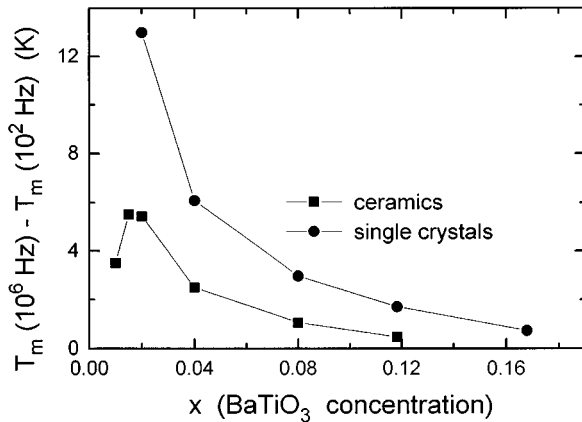


FIG. 5. Frequency dispersion of dielectric constant as a function of BaTiO_3 concentration x .

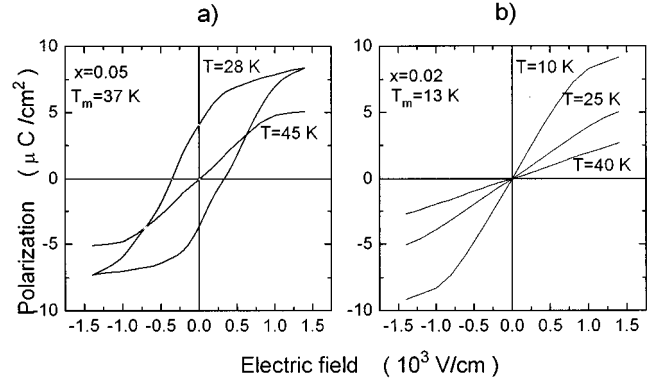


FIG. 6. Hysteresis loops $P(E)$ for ceramic samples with $x=0.05$ (a) and $x=0.02$ (b) at frequency of 50 Hz.

$T_a \approx 105$ K. To study this phase transition we used the ultrasonic method since a steplike anomaly of the ultrasonic velocity at T_a is known to be a good probe of the structural phase transition in SrTiO_3 . Figure 8 shows the temperature dependence of the velocity of longitudinal waves in the ceramic samples with different values of x . From the position of the velocity steplike anomaly one can determine the phase transition temperature T_a as a function of x .

IV. PHASE DIAGRAM

Using the dielectric and ultrasonic data presented in the preceding section we can construct the full phase diagram of the SrTiO_3 - BaTiO_3 system. This phase diagram is shown in Figs. 9 and 10. The temperature of the dielectric constant maximum T_m was taken as the ferroelectric phase transition temperature T_c . All the points in Figs. 9 and 10 refer to the cooling runs.

It is more convenient to discuss separately three different parts of this diagram for x in the ranges 1.0–0.15, 0.2–0.035, and 0.035–0.0.

A. $0.15 < x < 1.0$

This part of the phase diagram of the BaTiO_3 - SrTiO_3 solid solution, which is a textbook example of ferroelectric

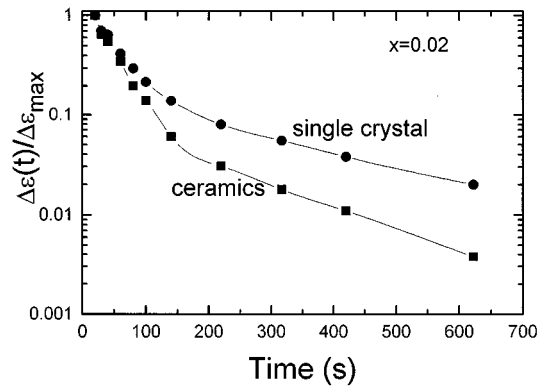


FIG. 7. Dielectric constant as a function of time in ceramics and single crystal with $x=0.02$, $T=10$ K, field cooling in $E_{dc}=1$ kV/cm. At $t=0$ E_{dc} is switched off. $\Delta\epsilon(t)/\Delta\epsilon_{max} = [\epsilon(t) - \epsilon_\infty]/(\epsilon_0 - \epsilon_\infty)$, where ϵ_0 and ϵ_∞ are the values of the dielectric constant at $t=0$ and ∞ , respectively.

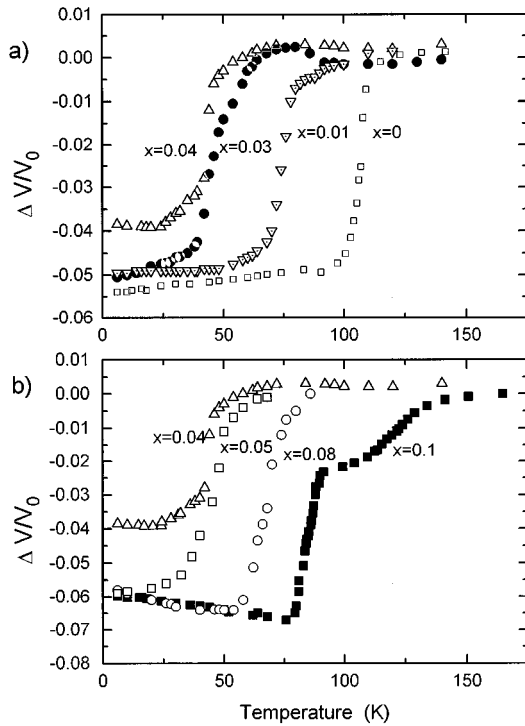


FIG. 8. Temperature dependence of the velocity of longitudinal ultrasonic waves with frequency 10 MHz in ceramic samples. (The numbers near the curves refer to BaTiO_3 concentration x .)

perovskite solid solutions, is well known, the most studied region of x being 0.3–1.0.^{1–3} Our results in general agree with the results published in the literature, so we highlight here only some points which have been paid little or no attention before.

As follows from Fig. 3 the temperature hysteresis for the $m3m$ - $4mm$ transition reduces to zero when x decreases from 1.0 down to 0.2–0.25. This means that when x goes down from $x=1.0$ the line of the first order phase transition in (T_c, x) plane transforms into the line of the second order phase transitions, with x near 0.2 being the tricritical point.

In this range of x a critical exponent γ in the relation $\varepsilon = C(T - T_0)^{-\gamma}$ is equal to 1; that is, the Curie-Weiss law is

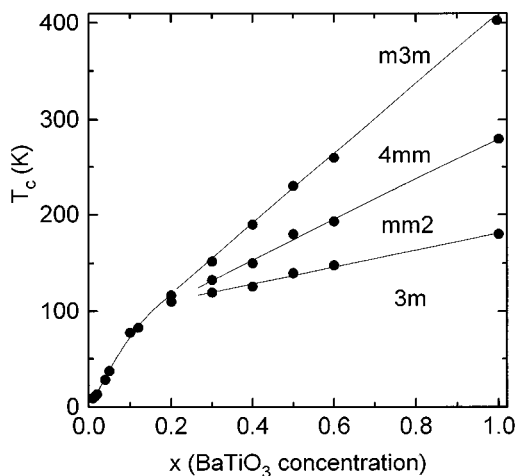


FIG. 9. Phase diagram of the $\text{Sr}_{1-x}\text{Ba}_x\text{TiO}_3$ system. The structural phase transition is not shown (see Fig. 10).

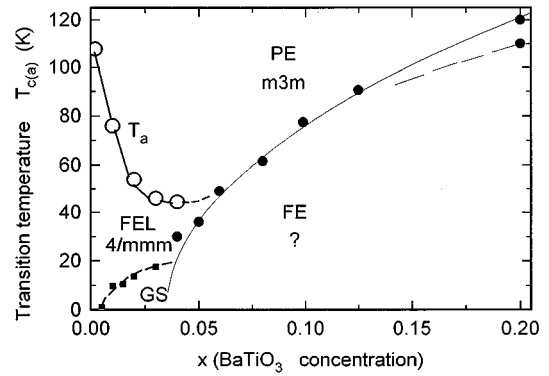


FIG. 10. Phase diagram of the $\text{Sr}_{1-x}\text{Ba}_x\text{TiO}_3$ system for low values of x . Solid line for T_c is the fitting of equation $T_c = A(x - x_c)^{1/2}$, where $A=300$ K and $x_c=0.035$ to the experimental points. PE, FE, FEL, and GS denote the paraelectric, the ferroelectric, the ferroelastic, and the glasslike state, respectively.

valid for $0.15 < x < 1.0$. The difference between T_c and the Curie-Weiss temperature T_0 is large for $x=1.0$ (about 13 K) and falls to zero at $x < 0.4$.

The next important point is a picture of the phase transitions in the vicinity of $x=0.15$. Though a final conclusion on this picture can be made only after precise x-ray measurements, we suppose that the most probable situation here is the following.

Three lines of the phase transitions in Fig. 9 converge in the region of x near 0.15, and at this point four phases are at equilibrium: the cubic $m3m$, the tetragonal $4mm$, the orthorhombic $mm2$, and the rhombohedral (trigonal) $3m$. This confluence does not contradict to the Gibbs phase rule, which says that when the number of parameters describing a system is equal to 3, as in our case (temperature, pressure, concentration), up to four phases can exist in the equilibrium.

B. $0.035 < x < 0.2$

This part of the phase diagram is shown in Fig. 10. The solid line in Fig. 10 obeys the relation $T_c = A(x - x_c)^{1/2}$ where $A=300$ K and $x_c=0.035$. As one can see there is a good fit of the experimental points to this relation.

The critical exponent γ at x near 0.2 is equal to 1 and then grows to about 1.5 when x decreases (Fig. 11). In this part of the diagram, as well as in the previous one, i.e., for x from 0.035 up to 1.0, one observes typical ferroelectric hysteresis loops at temperatures below $T_m = T_c$ [Fig. 6(a)]. The spontaneous polarization P_s for the ceramic sample with $x=0.05$ determined from the loop in Fig. 6(a) is $P_s=0.06$ C/m².

The peaks of the dielectric constant as a function of temperature are rather narrow for $x > 0.1$ and are very broad for $x < 0.1$. At the same time a frequency dispersion of the dielectric constant is launched at x near 0.15 and increases when x decreases (Fig. 5).

C. $0 < x < 0.035$

Figure 10 distinctly shows that the experimental points for T_c , which correspond to the temperature T_m of the dielectric constant maximum, form a specific branch in the phase diagram. From Fig. 1 it follows that for small x the maxima of

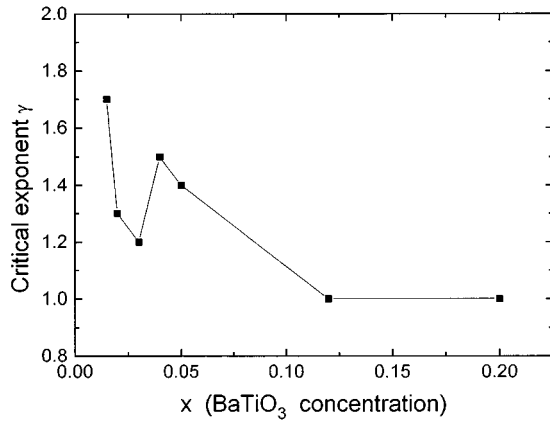


FIG. 11. Critical exponent γ in the temperature dependence of the dielectric constant, $\varepsilon = CT - T_0)^{-\gamma}$, as a function of BaTiO₃ concentration x .

the dielectric constant become very smooth and round and disappear completely at $x=0.005$.

Since no ferroelectric hysteresis loops were observed in samples with $x \leq 0.03$ at temperatures below T_m [Fig. 6(a)], one may conclude that in this range of x the temperature T_m does not correspond to a ferroelectric phase transition. Discussing this branch of the phase diagram, one should keep in mind that the temperature of the maxima of the dielectric constant depends strongly on frequency. This frequency dispersion is shown in Fig. 4 for $x=0.02$ and as a function of x in Fig. 5.

The critical exponent γ in the temperature dependence of the dielectric constant as a function of x is shown in Fig. 11. We estimate the accuracy of the determination of the critical exponent better than 10%. One can see that there is a non-monotonous behavior of the critical exponent, which for small x grows up to 1.7. Now we cannot explain this behavior, though one can say that it reflects in some way the transitions between different regions of the phase diagram.

As was shown in Sec. III, in field cooled samples with $x=0.02$ the long-term dielectric relaxation was observed at 10 K (Fig. 7). The dependence shown in Fig. 7 can be described by the relation

$$\varepsilon - \varepsilon_\infty = (\varepsilon_0 - \varepsilon_\infty) \exp(-t/\tau), \quad (1)$$

where ε , ε_0 , and ε_∞ are the values of the dielectric constant at times t , $t=0$, and $t=\infty$, respectively. The dc electric field is switched off at the moment $t=0$ after the field cooling run down to 10 K. It appears that the time dependence of ε is governed by two relaxation times: a fast relaxation with $\tau_1=60$ s and a slow relaxation with $\tau_2=300$ s. Such long relaxation times are typical ones for glasslike systems.¹⁰

Thus, in the Sr_{1-x}Ba_xTiO₃ system with $x \leq 0.03$ one observes the following features in the dielectric properties: the absence of any ferroelectric hysteresis loops below the temperature of the dielectric constant maximum T_m , a broad temperature dependence of the dielectric anomaly and its strong frequency dispersion, and the dependence of the dielectric constant on time after field cooling. All these experimental facts tell in favor of a glasslike behavior in the SrBaTiO₃ system at low temperatures and for small concentration of BaTiO₃.

It is now interesting to compare our results for this range of x ($0 < x < 0.035$) with those of Bednorz.⁶ Bednorz studied dielectric properties of Sr_{1-x}Ba_xTiO₃ single crystals with x value from 0 up to 0.016. For such low x we measured only ceramic samples, so we compare our results on ceramics with Bednorz data on single crystals. The dependence of T_m on x at low x in Fig. 10 is qualitatively similar to the results of Bednorz but our value of T_m is about 10 K lower. The reason of this discrepancy is not clear; in particular, it can be due to some uncontrolled impurities in raw materials. On the other hand, Bednorz, using only dielectric constant measurements at a single frequency, made a conclusion that at $x > 0.005$ there is a ferroelectric phase transition whereas we believe that this system is in a glasslike state at $0.005 < x < 0.035$.

D. Structural phase transition

The structural phase transition in SrTiO₃ single crystals has been extensively studied using ultrasonic methods.^{11,12} Our ultrasonic results on pure SrTiO₃ ceramic samples for longitudinal waves are in agreement with the results on single crystals.¹¹⁻¹³ In Fig. 8 one can see that the velocity jump at the phase transition point T_a amounts to 5%, which is more or less typical value for single crystals. The attenuation of the longitudinal waves at frequency of 10 MHz at temperatures below 100 K is about 10⁻¹ dB/cm. This small value shows that the scattering on ceramic grain boundaries is unimportant, and, moreover, the structural domains do not contribute to the attenuation.¹³ Both these features can be explained by the fact that the grain size in the ceramic samples (about 10⁻³ cm) is much smaller than the ultrasonic wavelength and is too small for the formation of structural domains in the individual grains.

From the ultrasonic results in Fig. 8 one can obtain the dependence of T_a on x . The transition temperature T_a is determined as a crossing point of a straight line extrapolation of the velocity temperature dependence at high temperatures and a line of a steepest slope of the steplike anomaly. From Fig. 8 it follows that when x increases from $x=0$ the steplike change of the velocity moves first towards lower temperatures [Fig. 8(a)] but a reverse movement begins above $x=0.05$ [Fig. 8(b)]. We think that this reverse movement is most likely due to the interference with the ferroelectric phase transition. In this region of x the structural and ferroelectric instabilities are almost at the same temperatures and it is difficult to determine the transition temperatures from Fig. 8(b). Therefore we used only the experimental data from Fig. 8(a) and obtained the structural phase transition line given in Fig. 10. For $x < 0.02$ there is a linear dependence of T_a on x with the slope $dT_a/dx = -25$ K/mol %. This value is about 40% larger than dT_a/dx obtained in Ref. 5 where single crystals with x equal to 0.006, 0.012, and 0.014 were measured at low frequencies.

At $x > 0.02$ the $T_a(x)$ dependence slows down and at x near 0.06, the structural phase transition line converges probably the ferroelectric phase transition line. Thus, in this range of x we have an interesting case when structural and ferroelectric instabilities are very close to each other and can even converge at a definite value of x .

TABLE I. Critical parameters x_c and r_c and relative change of ion sizes in KTaO_3 and SrTiO_3 with different impurities.

	$\Delta R/R$	x_c	r_c (Å)
$\text{KTaO}_3:\text{Li}$	+0.5	0.02	15
$\text{KTaO}_3:\text{Na}$	+0.3	0.12	8
$\text{KTaO}_3:\text{Nb}$	0.0	0.008	20
$\text{SrTiO}_3:\text{Ca}$	+0.1	0.0018	32
$\text{SrTiO}_3:\text{Ba}$	-0.2	0.035	12

V. DISCUSSION

The $\text{SrTiO}_3\text{-BaTiO}_3$ system appears to be very similar to the other systems based on the incipient ferroelectrics KTaO_3 and SrTiO_3 .^{10,14,15} This similarity is especially strong in the case of $\text{KTaO}_3\text{-KNbO}_3$ (KTN). The most common features of all these systems are the normal ferroelectric phase induced by an impurity with a large concentration x , the ferroelectric phase with a transition temperature which varies as $T_c = A(x - x_c)^{1/2}$ at medium concentration x , and the glass-like state at $x < x_c$. The relation $T_c = A(x - x_c)^{1/2}$ is typical of quantum ferroelectrics, $T_c = 0$ at $x = x_c$ being the quantum limit.^{10,14,15} It would be interesting to determine whether there is any correlation between the critical concentration x_c and the size of the ions.¹⁴

The experimental values of the critical concentration x_c for $\text{KTaO}_3\text{-LiTaO}_3$ (KTL),¹⁶ $\text{KTaO}_3\text{-NaTaO}_3$ (KTNa),¹⁷ $\text{KTaO}_3\text{-KNbO}_3$ (KTN),¹⁷ $\text{SrTiO}_3\text{-CaTaO}_3$ (STCa),¹⁸ and $\text{SrTiO}_3\text{-BaTiO}_3$ (SBT) (the present paper) are given in Table I. We define the critical radius r_c as $r_c = a/(x_c)^{1/3}$ where a is the lattice constant. The values of r_c are also given in Table I.

The critical concentration x_c and the critical radius r_c can be compared with the relative change of the ionic size $\Delta R = (R - R_i)/R$, where R is the radius of the host ion (K^+ or Sr^{2+}) and R_i is that of the impurity ion. From Table I it follows that there is no distinct correlation between r_c and $\Delta R/R$.

A widely accepted viewpoint now is that the behavior of the incipient ferroelectrics KTaO_3 and SrTiO_3 with impurities is determined by the off-center position of impurity ions (Li^+ , Na^+ , Nb^{5+} in KTaO_3 and Ca^{2+} in SrTiO_3). The dipole moment of the off-center ions and their reorientation rate are considered to be very important for the properties of the system in question. But this is not the case for $\text{SrTiO}_3:\text{Ba}^{2+}$, since the radius of Ba^{2+} ions (1.35 Å) is significantly larger than that of Sr^{2+} (1.13 Å). Thus the following question arises: is it really important to have off-center impurity ions for glasslike behavior in these systems?

An alternative to dipole moments of the off-center impurity ions could be quadrupole moments due to elastic strains induced by ion size mismatch. This mechanism is likely to be dominant at least for $\text{SrTiO}_3:\text{Ba}$, as well as, probably, for $\text{KTaO}_3:\text{Nb}$.¹⁶

The next interesting point is to compare our results on the dependence of T_c and T_a on x with hydrostatic pressure experiments in BaTiO_3 (Ref. 1) and SrTiO_3 .¹⁹

In the $\text{Sr}_{1-x}\text{Ba}_x\text{TiO}_3$ system the ferroelectric phase transition temperatures T_c decreases when x decreases, and the structural phase transition temperature T_a decreases when x increases. To compare the effect of a ‘‘chemical pressure’’ in the $\text{Sr}_{1-x}\text{Ba}_x\text{TiO}_3$ solid solution with the experimental results on the hydrostatic pressure effect on the phase transition temperatures, we can write the following relation:

$$dT_c/dx = (\partial T_c/\partial x)_V + (\partial T_c/\partial V)_x(\partial V/\partial x). \quad (2)$$

The second term in the right-hand side of Eq. (2) can be rewritten as

$$(\partial T_c/\partial V)_x(\partial V/\partial x) = -B(\partial T_c/\partial p)_x(1/V)(\partial V/\partial x), \quad (3)$$

where B is the bulk modulus. For BaTiO_3 $\partial T_c/\partial p$ is -6 , -3 , and 2.1 in 10^{-8} K/Pa for the phase transition $m3m\text{-}4mm$, $4mm\text{-}mm2$, and $mm2\text{-}3m$, respectively.

Our x-ray-diffraction data yield $\Delta a/a = 2.5 \times 10^{-2}x$ or $(1/V)(\partial V/\partial x) = 7.5 \times 10^{-2}$. Using $B = 1.7 \times 10^{11}$ Pa for pure BaTiO_3 and Eqs. (2) and (3) we can now calculate a volume contribution to dT_c/dx . The results are presented in Table II. In the first column of Table II the experimental values of dT_c/dx are given. The second column in the volume contribution calculated from Eq. (3) and the third one is $(\partial T_c/\partial x)_V$ which describes the pure effect of the solid solution composition for $V = \text{const}$ (a volume-independent contribution). The value of $(\partial T_c/\partial x)_V$ is obtained as a difference between the values given in the first and the second columns.

The same procedure can be used for the structural phase transition. It is known that the hydrostatic pressure increases the transition temperature T_a , with $\partial T_a/\partial p = 1.7 \times 10^{-8}$ K/Pa.¹⁹ Since the lattice volume of $\text{Sr}_{1-x}\text{Ba}_x\text{TiO}_3$ increases when x increases, the volume contribution to dT_a/dx should be negative which agrees with the sign of the experimental value of dT_a/dx . The volume-dependent and volume-independent contributions to dT_a/dx calculated using $B = 1.8 \times 10^{11}$ Pa for pure SrTiO_3 and Eqs. (2) and (3) are given in Table II.

The results presented in Table II show that the role of the volume-dependent effects and of the more complicated

TABLE II. Experimental values of $dT_{c(a)}/dx$ and volume-dependent and volume-independent contributions calculated from Eqs. (2) and (3).

Phase transition	$dT_{c(a)}/dx$ (K)	$(\partial T_{c(a)}/\partial V)_x(\partial V/\partial x)$ (K)	$(\partial T_{c(a)}/\partial x)_V$ (K)
$m3m\text{-}4mm$	3.6×10^2	7.6×10^2	-4.0×10^2
$4mm\text{-}mm2$	2×10^2	3.8×10^2	-1.8×10^2
$mm2\text{-}3m$	0.8×10^2	-2.6×10^2	3.4×10^2
$m3m\text{-}4/mmm$	-2.5×10^3	-2.3×10^2	-2.3×10^3

volume-independent effects is determined by the specific phase transition and can differ significantly for different phase transitions.

VI. CONCLUSIONS

The full phase diagram of the $\text{Sr}_{1-x}\text{Ba}_x\text{TiO}_3$ system has been derived from the dielectric and ultrasonic measurements. This system appears to behave similar to the other systems based on the incipient ferroelectrics KTaO_3 and SrTiO_3 . A small addition of Ba in SrTiO_3 (small x) induces a glasslike state, then at $x > x_c = 0.035$ a ferroelectric phase is induced with a transition temperature $T_c = A(x - x_c)^{1/2}$, where $A = 300$ K, and a further increase of x (> 0.2) leads to the normal ferroelectric phase transitions. At $x = 0.2 - 0.25$ a tricritical point in the phase diagram is observed where the $m3m$ - $4mm$ phase transition transforms from the first to the second order.

A complicated picture arises in the phase diagram near

$x = 0.15$. A multicritical point is possible here where three phase transition lines converge, and four phases are in equilibrium at one point in the (T, x) plane. Near to this point the structural phase transition line is also likely to converge with the ferroelectric transition line.

Our conjecture on a glasslike state at $x < 0.035$ is supported by a number of experimental observations: the absence of ferroelectric hysteresis loops, a frequency dispersion of the dielectric constant, and a time dependence of the dielectric constant after field cooling. In contrast to other similar systems, Ba^{2+} cannot be an off-center ion, since Ba^{2+} is larger than the Sr^{2+} host ion.

ACKNOWLEDGMENTS

We thank N. V. Zaitseva for the x-ray-diffraction measurements. The research described in this paper was made possible in part by Grant No. R3U300 from the International Science Foundation and Russian Government.

¹B. Jaffe, W. R. Cook, and H. Jaffe, *Piezoelectric Ceramics* (Academic, New York, 1971).

²M. E. Lines and A. M. Glass, *Principles and Applications of Ferroelectrics and Related Materials* (Clarendon, Oxford, 1977).

³G. A. Smolensky, V. A. Bokov, V. A. Isupov, N. N. Krainik, R. E. Pasynkov, A. I. Sokolov, and N. K. Yushin, *Ferroelectrics and Related Materials* (Gordon and Breach, New York, 1984).

⁴E. Hegenbarth, *Phys. Status Solidi* **9**, 191 (1965).

⁵S. Miura, M. Marutake, H. Unoki, H. Uwe, and T. Sakudo, *J. Phys. Soc. Jpn.* **38**, 1056 (1975).

⁶J. G. Bednorz, Ph.D. thesis, Swiss Federal Institute of Technology, Zürich, 1982.

⁷V. V. Lemanov, E. P. Smirnova, and E. A. Tarakanov, *Fiz. Tverd. Tela* **37**, 2476 (1995) [*Phys. Solid State* **37**, 1356 (1995)].

⁸K. A. Müller and H. Burkard, *Phys. Rev. B* **19**, 3593 (1979).

⁹L. Benguigui, *Phys. Status Solidi* **46a**, 337 (1978).

¹⁰W. Kleemann, *J. Mod. Phys. B* **7**, 2469 (1993).

¹¹W. Rehwald, *Solid State Commun.* **8**, 607 (1970).

¹²K. Fossheim and B. Berre, *Phys. Rev. B* **5**, 3292 (1972).

¹³E. V. Balashova, V. V. Lemanov, R. Kunze, G. Martin, and M. Weihnacht, *Solid State Commun.* **94**, 17 (1995).

¹⁴U. T. Höchli, K. Knorr, and A. Loidl, *Adv. Phys.* **39**, 405 (1990).

¹⁵B. E. Vugmeister and M. D. Glinchuk, *Rev. Mod. Phys.* **62**, 993 (1990).

¹⁶W. Kleemann and A. Kloessner, *Ferroelectrics* **150**, 35 (1993).

¹⁷D. Rytz, U. T. Höchli, and H. Bilz, *Phys. Rev. B* **22**, 359 (1980).

¹⁸J. G. Bednorz and K. A. Müller, *Phys. Rev. Lett.* **52**, 2289 (1984).

¹⁹G. Sorge, G. Schmidt, E. Hegenbarth, and C. H. Frenzel, *Phys. Status Solidi* **37**, K17 (1970).